

## Recent activities in neutron standardization at NMIJ/AIST

H. Harano, T. Matsumoto, T. Shimoyama, A. Uritani and K. Kudo

Quantum Radiation Division, National Metrology Institute of Japan (NMIJ),  
National Institute of Advanced Industrial Science and Technology (AIST), Japan

### 1. Introduction

This report described recent activities on neutron standardization at the National Metrology of Japan (NMIJ) at the National Institute of Advanced Industrial Science and Technology (AIST). The quality system has been established on neutron standards since April 2003. We have studied on a new type of neutron spectrometer [1], [2] and an NE213 scintillator [3] in relation to the standard field with the  ${}^9\text{Be}(\alpha,n){}^{12}\text{C}$  reaction being under construction. We have also carried out studies on characterization of gamma rays existing in NMIJ 5.0-MeV standard neutron field [4] and high-level technique for thermal-neutron measurement [5]. The members of the Neutron Standard Section are Katsuhisa KUDO (Head of Quantum Radiation Division), Yoshio HINO (Head of Radioactivity and Neutron Section), Hideki HARANO (Researcher), Tetsuro MATSUMOTO (Post Doctoral Fellow) and Tetsuya SHIMOYAMA (Part-Time Staff). Akira URITANI moved to the Nagoya University in this April.

### 2. Quality System (ISO17025)

The neutron standard section of NMIJ has established the quality system of neutron standards since April, 2003. We asked Drs. H. Klein (PTB), T. Aalbers (NMI), and T. Park (KRISS) to peer-review our quality system in September, 2003. We have obtained ISO17025 accreditation under the ASNITE (Accreditation System of the National Institute of Technology and Evaluation - National Metrology Institute) program for the following calibration services in last June. Table 1 gives quantity, calibration range and CMC of the neutron standards of NMIJ.

### 3. Fast Neutron Spectrometer Composed of PSPCs and Si(Li)-SSDs

In a neutron-calibration field it is necessary to experimentally evaluate a precise neutron spectrum in order to obtain the response function of a detector. We have standard fields of fast neutrons with energies of 5.0 MeV and 14.8 MeV. Then we have developed a fast neutron spectrometer with a recoil-proton method [1], [2]. We proposed to use charge-division-type position-sensitive proportional counters (PSPCs) and Si(Li) surface barrier detectors (Si(Li)-SSDs) in order to achieve excellent energy resolution.

Table 1: Quantity, calibration range and CMC of the neutron standards of NMIJ

Quantity	Calibration Range		Calibration and Measurement Capability ( $k=2$ )	
	Instrument or Artifact (Condition)	Measurand Level or Range		
Neutron	Neutron emission rate	Neutron source ( Am-Be )	$1 \times 10^3 \text{ s}^{-1} \sim 1 \times 10^7 \text{ s}^{-1}$	3.0 %
		Neutron source ( $^{252}\text{Cf}$ )	$1 \times 10^3 \text{ s}^{-1} \sim 1 \times 10^7 \text{ s}^{-1}$	3.2 %
	Thermal neutron fluence rate	Thermal neutron detectors	$5 \times 10 \text{ cm}^{-2}\text{s}^{-1} \sim 1 \times 10^4 \text{ cm}^{-2}\text{s}^{-1}$	2.8%
	Fast neutron fluence	Neutron detectors ( 144 keV )	$1 \times 10^3 \text{ cm}^{-2} \sim 1 \times 10^7 \text{ cm}^{-2}$	4.4 %
		Neutron detectors ( 565 keV )	$1 \times 10^3 \text{ cm}^{-2} \sim 1 \times 10^7 \text{ cm}^{-2}$	4.4%
		Neutron detectors ( 5.0 MeV )	$1 \times 10^3 \text{ cm}^{-2} \sim 1 \times 10^7 \text{ cm}^{-2}$	6.2 %
		Neutron detectors ( 14.8 MeV )	$1 \times 10^3 \text{ cm}^{-2} \sim 1 \times 10^7 \text{ cm}^{-2}$	3.2 %
		Neutron detectors ( Am-Be )	$1 \times 10^3 \text{ cm}^{-2} \sim 1 \times 10^7 \text{ cm}^{-2}$	2.8 %
		Neutron detectors ( $^{252}\text{Cf}$ )	$1 \times 10^3 \text{ cm}^{-2} \sim 1 \times 10^7 \text{ cm}^{-2}$	3.6 %

Figure 1 shows a schematic drawing of the present spectrometer. The spectrometer consists of the three PSPCs (P1-P3) with methane gas, the two Si(Li)-SSDs (50-360-2000SLM (Raytech Co.)) and the collimator made of polyethylene and lead. Recoil protons generated by interaction between a collimated incident neutron beam and hydrogen atoms in P1 pass through P2 and P3, and reach one of the Si(Li)-SSD. The recoil-proton energy is measured with the PSPCs and the of Si(Li)-SSD. At the same time, position signals at A and B in Figure 1 are obtained from the outputs of P2 and P3, and give the recoil angles. Finally, the neutron energy is derived from the recoil-proton energy and the recoil angle. This spectrometer was experimentally tested using a monoenergetic neutron beam with energy of 5.0 MeV produced from the  $\text{D}(\text{d},\text{n})^3\text{He}$  reaction with a deuteron beam from a 4-MV Pelletron accelerator. The energy resolution and the detection efficiency were 3.5 % and  $1.1 \times 10^{-3}$  %, respectively. The energy resolution better than 2 % could be achieved by selecting events under a proper condition. We also developed a Monte-Carlo code to evaluate the characteristics of the spectrometer. The results obtained from these simulations were in good agreement with those

obtained through experiments. This means that it is possible to predict the characteristics of the spectrometer under other experimental conditions by the simulation.

#### 4. Improvement of Photon Collection Uniformity from an NE213 Scintillator Using a Light Guide

The uniformity in collecting scintillation photons to the photomultiplier is one of the key parameters to carry out precise measurement using scintillators. A simple method is proposed to improve the collection uniformity of the scintillation photons just by inserting a light guide between a scintillator and a photomultiplier where the sidewall of the light guide is surrounded by a black paper as a photon absorber [3]. This light guide insertion is expected to have a function to reduce the collection efficiency of the scintillation photons generated closer to the photomultiplier due to the larger transmission loss, since a decrease of the angle of incidence raises the fraction of the photons escaping from the sidewall of the light guide. The effects of this method are examined experimentally using an NE213 scintillation detector. The NE213 scintillator is encapsulated in a cylindrical aluminum container, 50.8 mm inner diameter x 50.8 mm depth (inside), sealed with a Pyrex glass window as a viewing port. The scintillation photons from the window reach a photocathode of a photomultiplier tube (R329-02, Hamamatsu) directly or through a light guide connected with silicone grease (6262A, Oken). The light guide is an acrylic cylindrical disk 50.8 mm in diameter. A black paper to absorb the photons escaping from the surface surrounds the sidewall of the light guide. The housing is made of aluminum with an adjustable structure which allows the installation of the light guides of the thickness up to 30 mm. The photon collection uniformity was examined by measuring response spectra for a narrowly collimated <sup>137</sup>Cs gamma-ray beam 2 mm in diameter to irradiate selected portions of the NE213 scintillator. The gamma-ray beam impinged perpendicularly on the sidewall toward the central axis of the scintillator. The distance between the beamline and the NE213 front face was set to 5, 15, 25, 35 and 45 mm. The measured spectra were compared to the response function calculated for the above condition by the EGS4 electron-photon transport

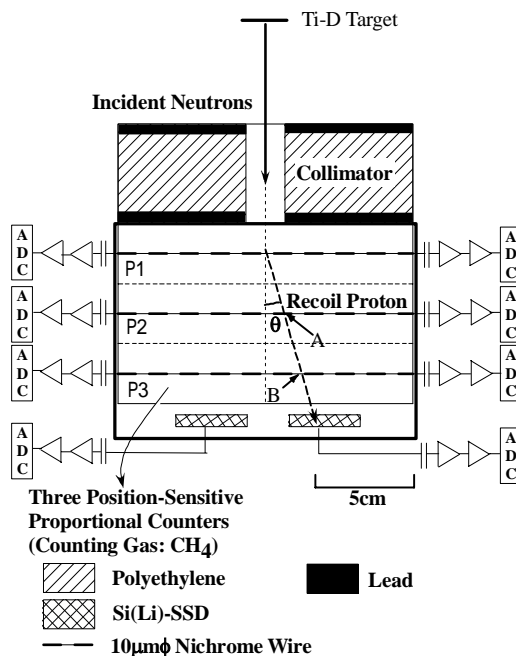


Figure 1: Schematic drawing of the fast neutron spectrometer

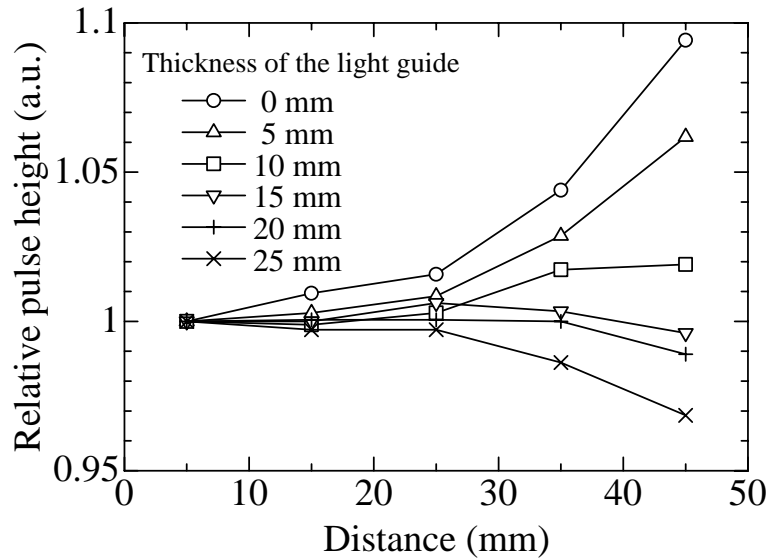


Figure 2 Relative pulse height corresponding to the Compton edge.

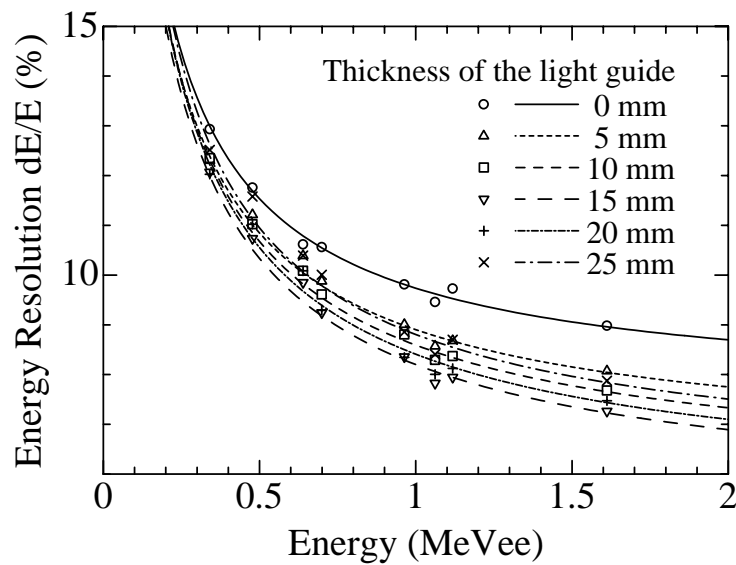


Figure 3 Energy resolutions  $dE/E$  (%) obtained at the Compton edges.

Monte-Carlo code [6] and the corresponding channel and the resolution were determined at the energy of the Compton edge. Figure 2 summarizes the relations between the Compton-edge channels and the gamma-ray beam positions for the different thickness of the light guide. For the direct coupling without the light guide, the collection efficiency appeared to be higher in those regions closer to the photocathode. This tendency was compensated by inserting the 10 to 20 mm thick light guide. It became however worse again for the thicker light guides. The light propagation was simulated to see what took place in the scintillator and the light guide using the ray-tracing program GuideM [7]. Energy resolutions were evaluated for the irradiation to the side of

the scintillator with the uncollimated gamma rays from reference sources of  $^{88}\text{Y}$ ,  $^{60}\text{Co}$ ,  $^{22}\text{Na}$ ,  $^{54}\text{Mn}$ , and  $^{137}\text{Cs}$  for the different thickness of the light guide. The gamma-ray sources were located 15 cm apart from the NE213 central axis. The energy resolutions at the Compton edges are summarized in Figure 3. The configuration with the 15 mm thick light guide shows the best energy resolution. The capability of the pulse shape discrimination between gamma rays and neutrons was also examined using a  $^{252}\text{Cf}$  source. It was confirmed that the light guide insertion introduced no significant degradation in the discrimination capability. We will apply the NE213 detector employing this technique for the determination of the neutron fluence at the national standard field (1.16-13.37 MeV,  $^9\text{Be}(\alpha,n)^{12}\text{C}$ ) under development at NMIJ/AIST.

### 5. Characterization of Gamma Rays Existing in NMIJ 5.0 MeV Standard Neutron Field

Neutron fields are always accompanied by gamma rays produced in neutron sources and surroundings. It is very important to quantitatively characterize these parasite gamma rays for calibration of neutron detectors or sensing elements, because most of them are sensitive to both neutrons and gamma rays. We have characterized the parasite gamma rays in the thermal neutron field [8], but not so much efforts have been taken for the fast neutron field. In the present study, we characterized these gamma rays in the 5.0 MeV standard neutron field [4].

The 4-MV Pelletron accelerator (National Electrostatic, USA) is used to produce the 5.0 MeV neutrons by the  $\text{D}(\text{d},\text{n})^3\text{He}$  reaction, where 1.817 MeV deuteron beam impinges on the target consisting of Ti-D evaporated on a 0.5 mm thick copper backing. The mixed photon dose in the fast neutron field was measured with the NE213 liquid organic scintillation detector, 5.08 cm diameter x 5.08 cm thick, coupled to a photomultiplier tube (R329-02, Hamamatsu). The pulse shape discrimination between gamma rays and neutrons was performed using the differences in the rise time. The irradiated neutron fluence was determined at the calibration point with the count of a polyethylene long counter (PLC) situated at the angle of 45 degree.

The gamma-ray response spectra of the NE213 detector were measured using gamma-ray reference sources of  $^{88}\text{Y}$ ,  $^{60}\text{Co}$ ,  $^{22}\text{Na}$ ,  $^{54}\text{Mn}$ , and  $^{137}\text{Cs}$ . The measured spectra were compared to the response function calculated for the above condition by the EGS4 electron-photon transport Monte-Carlo code [6] and the corresponding channel and the resolution were determined at the energy of the Compton edge. The response functions were prepared by calculating and tallying the energy deposition in the NE213 detector for the incident gamma rays up to 10 MeV by the EGS4 code. The response matrix for the unfolding codes was completed by folding these calculated response functions with the Gaussian distribution.

Figure 4 shows the pulse height spectra measured in the 5.0 MeV standard neutron field. The NE213 detector was located at 50 cm and 100 cm from the target. Figure 5 shows the unfolded spectra obtained by the MIEKE code in the HEPRO program package [9]. The effective dose

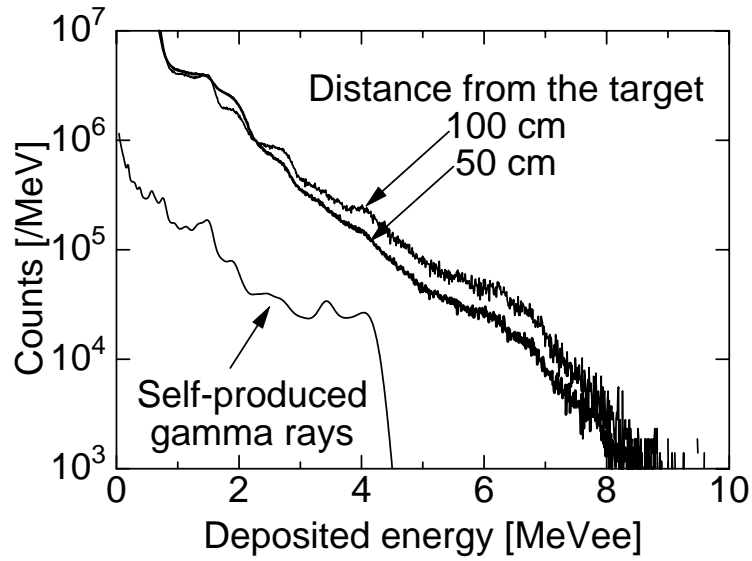


Figure 4 Pulse height spectra measured in the 5.0 MeV standard neutron field and calculated response to the neutron-induced gamma rays in the detector.

Table 2 Effective dose equivalents of the gamma rays at  $10^7$  n/cm<sup>2</sup> on the detector.

Position	Effective dose (Corrected)	
	AP [ $\mu$ Sv]	LAT [ $\mu$ Sv]
50 cm	26.0 (24.1)	20.2 (18.9)
100 cm	29.2 (27.2)	22.7 (21.3)

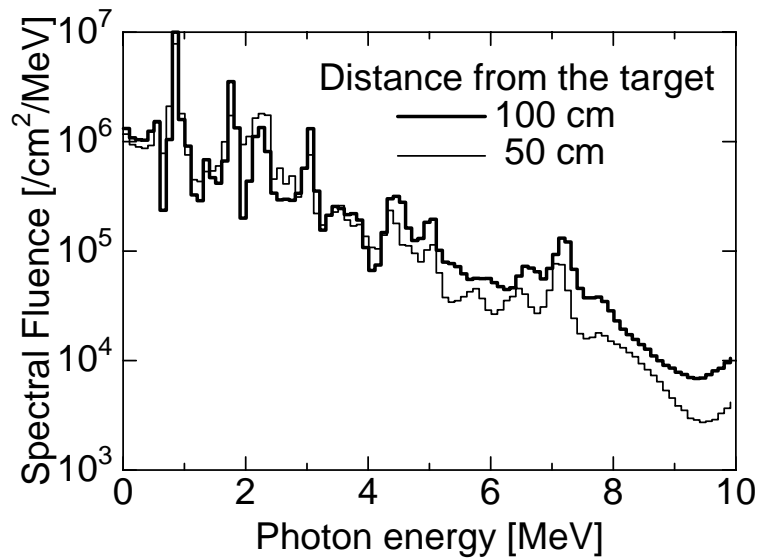


Figure 5 Photon energy spectra in the 5.0 MeV standard neutron field unfolded by the MIEKE code.

equivalents were evaluated for these spectral fluences using the conversion coefficients calculated for the MIRD phantoms [10]. Table 2 summarizes the results for the AP geometry (irradiation from the front to the back) and the LAT geometry (lateral irradiation from either side). These values however include the contribution of the neutron-induced gamma rays generated in the detector assembly. Figure 1 also shows the detector response to the self-produced gamma rays calculated using the MCNP4C code [11]. The corrected values of the effective dose equivalent are also shown in Table 1.

Further characterization is in progress on the parasite gamma rays existing in the fast neutron field of the other energies such as 144 keV, 565 keV and 14.8 MeV. We will measure the response spectra for the gamma rays above 1.6 MeV using laser Compton scattered (LCS) photon beams to estimate the nonlinearity of the detector output and increase the accuracy of analysis as the next step.

## 6. Development of a Tiny Neutron Prob with an Optical Fiber

A monitor of a thermal neutron flux is important for boron neutron capture therapy (BNCT) [12]. Then, we have developed a tiny neutron probe detector with an optical fiber that is used for transmission of scintillation light from a neutron probe [5]. We use  ${}^6\text{LiF}$  that works as a neutron converter and a film-like  $\text{ZnS(Ag)}$  scintillator that is  $25\ \mu\text{m}$  thick on a cellulose acetate sheet  $12\ \mu\text{m}$  thick. The neutron probe is made by evaporating  ${}^6\text{LiF}$  powder onto a cellulose side of the scintillator. The neutron probe is stick on an optical fiber end (detector A). Another end is connected to a photomultiplier that follows a pre-amplifier and a linear amplifier. In order to improve neutron sensitivity, we have newly made another neutron probe with a wavelength shifting (WLS) fiber [13]. In this type, the  $\text{ZnS(Ag)}$  sheet with  ${}^6\text{LiF}$  is attached on the side surface of the WLS fiber whose length is 1 cm (detector B). In the present study, characteristics of the two detectors are evaluated experimentally.

Thermal neutrons used in this study were given from the heavy water neutron irradiation facility at the Kyoto University Reactor. A gold-activation method determined the thermal neutron flux, which was of the order of  $10^{-5}\ \text{cm}^{-2}\cdot\text{s}^{-1}$ .

The pulse-height spectrum (PHS) measured with detector A is shown in Figure 6(a). This PHS indicates the high neutron-gamma discrimination ability. Alpha particles from the  ${}^6\text{LiF}$  neutron converter were never detected and only tritons

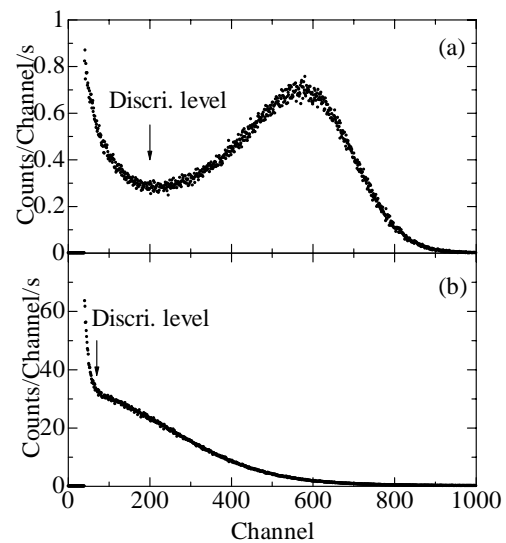


**Figure6:** PHS measured with (a) detector A and (b) detector B.

contributed to the PHS, because the cellulose acetate sheet fully stopped the alpha particles. As the result, the peak of the neutron events appears clearly as shown in Figure 1. It is easy to set the discrimination level at the valley. The sensitivity of detector A was  $2.1 \times 10^{-3} \text{ cm}^2$ .

The PHS measured with detector B is shown in Figure 6(b). The gain of the amplifier was 10 times higher than that applied for detector A, because the intensity of the scintillation light decreased during the process of wavelength shifting. The sensitivity of detector B was  $9.5 \times 10^{-2} \text{ cm}^2$ , when the discrimination level was set at 70 ch.. The sensitivity of detector B was 40 times higher than that of detector A at the sacrifice of the neutron-gamma discrimination ability and the spatial resolution. The spatial resolution became worse because of the long neutron probe.

### References:

1. T. Matsumoto, H. Harano, Y. Ito, A. Uritani, K. Emi and K. Kudo; “*Development of Fast Neutron Spectrometer Composed of Silicon-SSD and Position-Sensitive Proportional Counters*”, *Radiat. Prot. Dosim.*, **110**, 223-226 (2004).
2. T. Matsumoto, H. Harano, A. Uritani and K. Kudo; “*Fast Neutron Spectrometer Composed PSPCs and Si(Li)-SSDs with Excellent Energy Resolution and Detection Efficiency*”, *IEEE Trans. Nucl. Sci.* (Submitted).
3. H. Harano, T. Matsumoto, Y. Shibata, Y. Ito, A. Uritani and K. Kudo; “*Improvement of Photon Collection Uniformity from an NE213 Scintillator Using a Light Guide*”, *IEEE Trans. Nucl. Sci.* (Submitted).
4. H. Harano, T. Matsumoto, Y. Ito, A. Uritani and K. Kudo; “*Characterization of Gamma Rays Existing in the NMIJ Standard Neutron Field*”, *Radiat. Prot. Dosim.*, **110**, 69-72 (2004).
5. Y. Ito, G. Katano, H. Harano, T. Matsumoto, A. Uritani, K. Kudo, K. Kobayashi, T. Yoshimoto, Y. Sakurai, T. Kobayashi and C. Mori; “*Development of a Tiny Neutron Probe with an Optical Fiber for BNCT*”, *Radiat. Prot. Dosim.*, **110**, 619-622(2004).
6. W.R.Nelson, H. Hirayama and D. W. O. Rogers; “*The EGS4 Code System*”, SLAC-265, Stanford University (1985).
7. downloadable at <http://www.npl.uiuc.edu/exp/G0/detectors/detectors.html>
8. K. Kudo, N. Takeda, S. Koshikawa, H. Toyokawa, H. Ohgaki and M. Matzke; “*Photon Spectrometry in Thermal Neutron Standard Field*”, *Nucl. Instr. Meth.* A476, 213-217 (2002).
9. M. Matzke; “*Unfolding of Pulse Height Spectra: The HEPRO Program System*”, PTB Report PTB-N-19, Braunschweig (1994).
10. ICRP Data for use in protection against external radiation. ICRP Publication 51 Ann. ICRP 17(2/3) (Oxford: Pergamon Press) (1987).
11. J. F. Briesmeister Ed.; “*A General Monte Carlo n-Particle Transport Code, Version 4C*”, LA-13709-M (Los Alamos National Laboratory, Los Alamos, NM) (2000).



12. Y. Sakurai and T. Kobayashi; “*Characteristics of the KUR Heavy Water Neutron Irradiation Field with Variable Energy Spectra*”, *Nucl. Instr. Meth.* **A453**, 569-596 (2000).
13. A. Gorin, K. Kuroda, I. Manuilov, K. Morimoto, T. Oku, A. Ryazantsev, M. H. Shimizu, J. Suzuki and F. Tokanai; “*Development of Scintillation Imaging Device for Cold Neutrons*” *Nucl. Instr. Meth.* **A479**, 456-460 (2002).